The New Short-Lived Isotope ^{221}U and the Mass-Surface Near $N = 126$

J. Khuyagbaatar,[1,2,*] A. Yakushev,[2] Ch.E. Düllmann,[1,2,3] D. Ackermann,[2,†] L.-L. Andersson,[1] M. Block,[1,2,3] H. Brand,[2] D.M. Cox,[4] J. Even,[1,‡] U. Forsberg,[5] P. Golubev,[5] W. Hartmann,[2] R.-D. Herzberg,[4] F.P. Heßberger,[1,2] J. Hoffmann,[2] A. Hübner,[2] E. Jäger,[2] J. Jeppsson,[5] B. Kindler,[2] J.V. Kratz,[3] J. Krier,[2] N. Kurz,[2] B. Lommel,[2] M. Maiti,[6,§] S. Minami,[2] A.K. Mistry,[4] Ch.M. Mrosek,[3] I. Pysmenetska,[2] D. Rudolph,[5] L.G. Sarmiento,[5] H. Schaffner,[2] M. Schädel,[2] B. Schausten,[2] J. Steiner,[2] T. Torres De Heidenreich,[2] J. Uusitalo,[7] M. Wegrzecki,[8] N. Wiehl,[1,3] and V. Yakusheva[1]

[1] *Helmholtz Institute Mainz, 55099 Mainz, Germany*
[2] *GSI Helmholtzzentrum für Schwerionenforschung, 64291 Darmstadt, Germany*
[3] *Johannes Gutenberg-Universität Mainz, 55099 Mainz, Germany*
[4] *University of Liverpool, Liverpool L69 7ZE, United Kingdom*
[5] *Lund University, 22100 Lund, Sweden*
[6] *Saha Institute of Nuclear Physics, Kolkata 700064, India*
[7] *University of Jyväskylä, 40351 Jyväskylä, Finland*
[8] *The Institute of Electron Technology, 02-668 Warsaw, Poland*

(Dated: October 2, 2015)

Two short-lived isotopes ^{221}U and ^{222}U were produced as evaporation residues of the fusion reaction ^{50}Ti + ^{176}Yb at the gas-filled recoil separator TASCA. An α decay with an energy of $E_\alpha = 9.31(5)$ MeV and half-life $T_{1/2} = 4.7(7)\,\mu$s was attributed to ^{222}U. The new isotope ^{221}U was identified by its α decay with $E_\alpha = 9.71(5)$ MeV and $T_{1/2} = 0.66(14)\,\mu$s. Synthesis and detection of these unstable heavy nuclei and their descendants were achieved thanks to a fast data read-out system. The evolution of the $N = 126$ shell closure and its influence on the stability of uranium isotopes are discussed within the framework of α-decay reduced width.

PACS numbers: 23.60.+e, 27.90.+b, 25.70.Jj

The shell structure of the atomic nucleus is one of the fundamental pillars of nature. As one consequence, the spherically-shaped nuclei with fully-filled proton and neutron shells at $Z, N = 2$, 8, 20, 28, 50, 82 and $N = 126$ have enhanced stability against any type of ground-state radioactive decay (alpha, beta, fission etc.) [1, 2]. Our current understanding of the shell structure is well established, best in case of nuclei along the valley of stability, but also for artificially synthesized nuclei. However, currently available experimental techniques limit access to nuclei in extreme regions where theoretical descriptions of nuclear matter can be tested [2–4]. One such region is located upwards along $N = 126$ towards higher Z above Pa ($Z = 91$), where the evolution of the shell closure is yet poorly examined.

To this end, only a limited amount of experimental observables like the α-decay energy, Q_α, and half-life, $T_{1/2}$, are available to date. Systematic analyses of these macroscopic observables along the isotopic chain (i.e., nuclei with the same Z) provide evidence of the $N = 126$ shell closure. More detailed information on nuclear structure and stability can be obtained from the α-particle preformation probability inside the nucleus [5] which microscopically quantifies the stability against α decay. Different variables equivalent to the α-particle preformation probability in which both Q_α and $T_{1/2}$ are simultaneously involved, can be deduced within different quantum-mechanical approaches [6, 7]. Commonly, a reduced width for α decay, δ^2 [6], which takes into account the angular momentum of the emitted α particle, is used.

At and below $N = 126$, reduced widths of isotones of Po ($Z = 84$) to Pa are significantly lower than those of the $N = 128$-130 isotones located beyond the closed $N = 126$ shell [6–8]. This reflects the robustness of the $N = 126$ shell closure up to Pa and the effect of the semi-magic nucleus core with $N = 126$. The evolution of this closure towards higher Z is yet unknown due to the absence of data on U isotopes with $N = 128$-130. U isotopes with $N = 124$-127 and $N \geq 131$ are known by their α decay [9–11]. For ^{222}U ($N = 130$) only a half-life of $T_{1/2} = 1.0^{+1.2}_{-0.4}\,\mu$s was deduced from the observation of just three events [12]. The α-decay energies could not be deduced as a result of the signals being summed (pile-up) with those of the rapidly-following α decays of the ^{218}Th daughter ($T_{1/2} = 0.117(9)\,\mu$s [9]).

Generally the synthesis and the detection of neutron-deficient isotopes of U (as well as heavier elements) from this region are challenging due to their low production rates and short half-lives, which may limit their identification [12, 13]. An additional difficulty arises from the fusion reaction itself, as the compound nucleus fission and the evaporation of protons and/or α particles is by far dominant over neutron evaporation in the early

* J.Khuyagbaatar@gsi.de
† Present address: GANIL, CEA/DSM-CNRS/IN2P3, Bd Henri Becquerel, BP 55027, F-14076 Caen Cedex 5, France
‡ Present address: TRIUMF, 4004 Wesbrook Mall Vancouver, BC, V6T 2A3, Canada
§ Present address: Indian Institute of Technology Roorkee, Roorkee 247667, India.

stages of de-excitation [13]. Thus, no new or improved data in this region of sub-μs isotopes carrying information on the $N = 126$ shell closure of elements above Pa have been measured in the last thirty years.

In this paper, we report the first identification of the isotope ^{221}U and new data for ^{222}U. The known data on Po-U are discussed by means of α-decay systematics and thus help shedding light on the evolution of the $N = 126$ shell closure in U.

The experiment was carried out at the GSI Helmholtzzentrum für Schwerionenforschung, Darmstadt, Germany. The isotopes ^{221}U and ^{222}U were produced in the ^{50}Ti + ^{176}Yb reaction at the gas-filled Trans-Actinide Separator and Chemistry Apparatus (TASCA) [14, 15]. A pulsed (5 ms beam-on and 15 ms beam-off) ^{50}Ti^{12+} beam was accelerated by the UNIversal Linear ACcelerator (UNILAC) to energies in the range of 231–255 MeV in the center of the ^{176}Yb targets. These correspond to excitation energies of 40–60 MeV in ^{226}U* where maxima of $4n$ (^{222}U) and $5n$ (^{221}U) evaporation channels are predicted to occur according to the statistical fusion-evaporation code HIVAP [16]. Four target segments with average thickness of 0.45(5) mg/cm^2 were mounted on a wheel which rotates synchronously to the beam pulses [17]. The magnets of TASCA were set to guide the evaporation residues (ERs) ^{221}U and ^{222}U with a magnetic rigidity of 1.66 Tm [18–20] to the center of the focal plane with an estimated efficiency of 50(5)%. The time of flight of ^{221,222}U ERs through TASCA was estimated to be 0.53(6) μs.

ERs that do not decay in flight (through TASCA) were implanted into a double-sided silicon strip "stop detector" with 144 vertical and 48 horizontal 1-mm wide strips. A multiwire proportional counter (MWPC) was mounted in front of the stop detector to distinguish the genuine radioactive decay of implanted ERs from beam-related events. A detailed description of the TASCA focal plane detector is given in [15].

Signals from all the detectors were processed in a Combined ANalog and DIgital (CANDI) data acquisition system comprising analog and digital branches. The signals from the 48 horizontal strips (n-side) were recorded in 50 μs-long traces by 60 MHz-sampling ADCs [21]. The traces were selected to be longer than the dead time of the analog branch of $\approx$35 μs. Energy resolutions (FWHM) of individual horizontal strips of the stop detector coupled to the analog branch were about 60 keV for 8.7-MeV α particles. The amplitudes, i.e., energy of signals (n-side) stored in traces were extracted by using different types of software algorithms depending on the multiplicity of the recorded signals [22]. The best resolutions, about 70 keV were achieved for 8.7-MeV α particles that were registered as single events in the traces. The best energy resolutions of multiple α events stored in a single trace with time differences down to 1 μs and 0.17 μs were $\approx$110 keV and $\approx$180 keV, respectively.

Half-lives known for ^{222}U and its daughter ^{218}Th and predicted for ^{221}U are much shorter [9] than the 50 μs

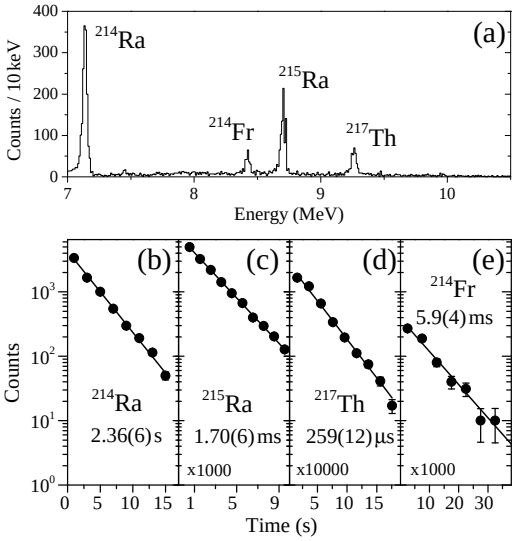

FIG. 1. Results from a correlation analysis of the type ER–α within 20 s: (a) spectrum of correlated α-particles registered at a bombarding energy of 239 MeV and (b-d) total decay curves of the implanted nuclei. (e) Decay curve of ^{214}Fr identified in correlation analysis of type ER–α(7-18 MeV)–α(^{214}Fr).

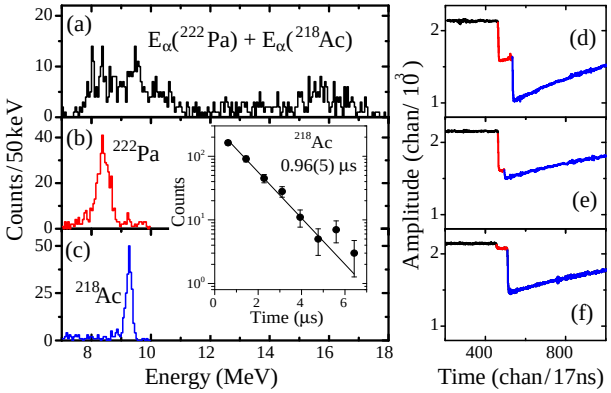

FIG. 2. (color online) Identification spectra for the separation of pile-up events originating from the decay chains ER-α(7-18 MeV)-α(^{214}Fr). (a) Energy spectrum from the analog part of the data. (b) and (c) energy spectra of events deduced from the digital traces. Examples of some pile-up traces: (d) two α particles with full energies, (e) and (f) for traces where the second and first α particle respectively, escaped in the backward direction and deposited only partial energy in the stop detector.

trace-length of CANDI. Thus, their radioactive decay signature is registered in digital traces of implantation signals (ER-like). The analysis procedure thus consists of two main steps:

i) A correlation analysis of the analog data, searching for ER–α chains requiring that both the ER-like and the α-like events (7-18 MeV) occurred in the same pixel of the stop detector within 20 s. The results of the correlation analysis are shown in Fig. 1. The implantation of ^{214}Ra, ^{215}Ra, ^{217}Th, and ^{214}Fr was identified by their known α-decay properties [9], and the corresponding ERs were

assigned for each event.

ii) Traces of all ERs correlated to a subsequent α decay of ^{214}Ra and ^{217}Th, which are members of the α-decay chains originating from ^{222}U and ^{221}U, respectively, were checked event by event for the presence of multiple signals.

In case of ^{217}Th and ^{214}Fr, an additional correlation analysis ER–α–α was performed to reconstruct the full pattern of the α-decay chain. As an example, ^{214}Fr was found to be the last member of the ER–α(7-18 MeV)–α(^{214}Fr) chain with $T_{1/2} = 5.9(4)$ ms (See Fig. 1). An energy spectrum (analog branch) of the second member with $T_{1/2} = 3.5(1)$ ms is shown in Fig. 2 (a). To resolve apparent pile-up events, the digital traces were analysed in the second step. Different examples of such events are presented in Fig. 2 (d-f). The energy spectra of the two signals allowed the separate peaks to be clearly resolved, which correspond to known α-decay energies of ^{222}Pa and ^{218}Ac [9]. Time differences between those signals yield $T_{1/2} = 0.96(5)\mu$s, which agrees well with the literature data of ^{218}Ac [9]. Thus, the origin of the α-decay of ^{214}Fr was attributed to the implantation of ^{222}Pa produced as an ER via the $p3n$ de-excitation channel from the compound nucleus ^{226}U*. The same digital-trace analysis was used for the extraction of α-decay properties of all other short-lived nuclei.

Significant amounts of ER traces correlated to α(^{215}Ra) were stored with double signals. A resolved energy spectrum of the second signal and the decay curve extracted from the time difference of these signals (shown in Fig. 3) is in good agreement with literature data for ^{219}Th [9]. No triple signals which would correspond to the implantation of ^{223}U ($T_{1/2} = 55(10)\,\mu$s [9]) from the $3n$ channel were detected.

Traces with two and three signals were detected for ERs followed by α(^{214}Ra). Traces with two signals and with very short time differences leading to $T_{1/2} = 0.16(4)\,\mu$s (see Fig. 3) between the signals were assigned to the implantation and α decay of ^{218}Th ($T_{1/2} = 0.117(9)\,\mu$s [9]) produced in the $\alpha 4n$ channel.

Eighty-one ER traces containing three signals were unambiguously attributed to the implantation of ^{222}U followed by α decays of ^{222}U and ^{218}Th. One such trace is shown in Fig. 4. A half-life of 4.7(7) μs and an energy of 9.31(5) MeV were deduced for the α decay of ^{222}U (see Fig. 3).

Twenty-six ER traces followed by subsequent α decays of ^{217}Th and ^{213}Ra were stored with double signals and are attributed to the implantation and α decay of the hitherto unknown ^{221}U (see Fig. 4). A half-life of 0.66(14) μs and an α-particle energy of 9.71(5) MeV were deduced (see Fig. 3) for this isotope.

The most favoured α transitions in nuclei with $N = 129$ proceed through the same $\nu 2g_{9/2}$ orbital in the mother and daughter nuclei. Thus, the observed α decay in ^{221}U is attributed to such a transition. The $(9/2^+)$ state is tentatively assigned to the ground state of ^{221}U based on systematics [9, 10]. Alpha decays of both ^{221}U and ^{222}U

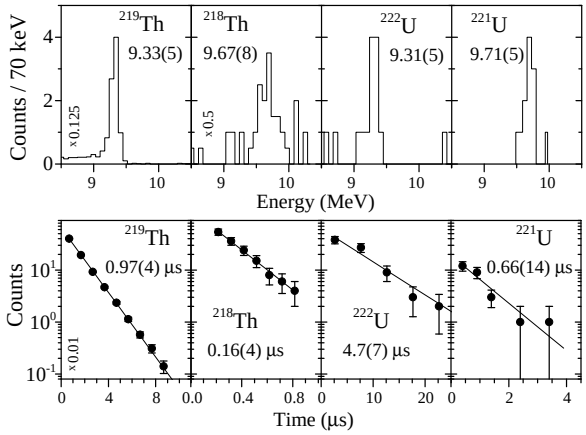

FIG. 3. Energy spectra and decay curves of α particles emitted from ^{219}Th, ^{218}Th, ^{222}U and ^{221}U. The data were extracted from the digital data branch. In case of ^{218}Th both double and triple-signaled traces from ER–α(^{214}Ra) were used. All traces with time differences down to 100 ns between the preceding signal and α decay were used.

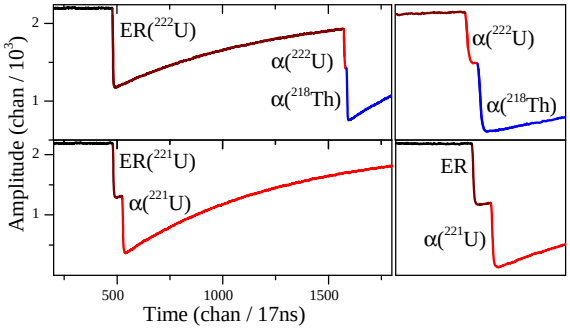

FIG. 4. (color online) Examples of traces where ^{222}U and ^{221}U were registered. Right-panel: enlarged figures of rapidly correlated signals.

are in good agreement with Q_α [23] and $T_{1/2}$ systematics [10].

The new α-decay data on ^{221}U and ^{222}U isotopes together with literature values ([9, 11]) allow us to construct the tendencies of δ^2 in the N =129, 130 isotones up to U, where the $\pi(1h_{9/2})$ orbital is fully-filled. The deduced δ^2-values of N =124,126-130 isotones are shown in Fig. 5. In the case of the N =129 isotones, only α transitions populating the same single-neutron states ($\Delta\ell = 0$) in the daughter nuclei were taken, and for the cases at $N = 127$, where $\Delta\ell = 5$ arises from the difference of the initial $\nu(2g_{9/2})^1$ and final $\nu(3p_{1/2})^{-1}$ configurations, is used.

Up to Th ($Z = 90$), the δ^2-values of $N = 124$,128-130 isotones are larger than the $N = 126$,127 ones, which clearly shows a strong effect of the $N = 126$ shell closure. At the same time the δ^2-values of $N = 126$,127 isotones, which are known up to U, smoothly rise with increasing Z, indicating a weakening of the semi-magic core with $N = 126$. For $N = 129$,130 isotones, where our new data allow extending the systematics up to U, the δ^2-values decrease in contrast to the trend seen in the $N = 126$,127

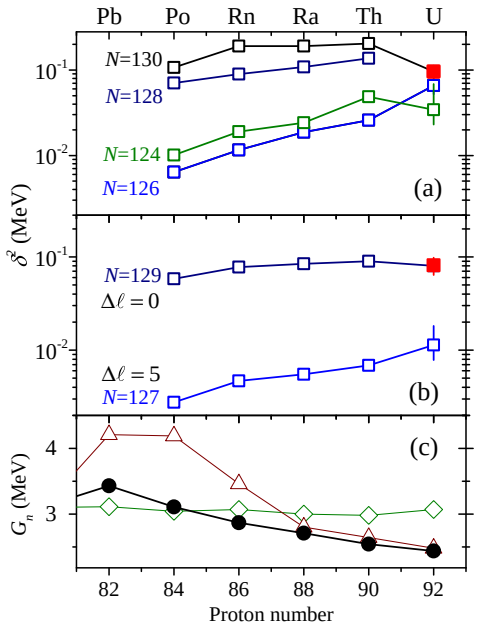

FIG. 5. (color online) Reduced α-decay widths (δ^2, [6]) of even-A (a) and odd-A (b) isotopes, and (c) neutron-shell gaps (G_n, [2]) of Po-U as function of the Z. Errors originating solely from half-lives are given for U. (c) Experimental data (full dots) [23] are compared to FRDM95 (open diamonds) [24] and HFB26 (open triangles) [25] calculations. See text for details.

isotones. The sudden increase of δ^2-values when crossing the $N=126$ shell closure seen in lighter elements with even-A is no longer present at $Z=92$. In odd-A nuclei the gap is still persisting at $Z=92$, in contrast to the even-A case. Essentially α-decay of the even-even nuclei, where all nucleons are paired provide better information on their structure compared to odd-A ones, where α-decay is strongly influenced by their unpaired nucleon.

The above observed feature for even-A nuclei indicates a weakening of the $N=126$ shell stabilization effect for U, which can be inferred even in the absence of data on ^{220}U ($N=128$). In addition δ^2-values of $N=124$ isotones show again a notable discrepancy in U. The smallest δ^2-value is found in ^{216}U ($N=124$), which can be argued as having a more stabilized core than the semi-magic ^{218}U ($N=126$).

A weakening of the $N=126$ shell closure can also be seen in the reduction of the neutron-shell gap in elements above Pb ($Z=82$). The neutron-shell gap, G_n, between the last-occupied and first-valence orbitals around $N=126$ can be calculated as

$$G_n(Z,126) = 2B(Z,126) - B(Z,125) - B(Z,127) \quad (1)$$

using the known (except ^{217}U) binding energies, B [2, 23]. These gaps are shown in Fig. 5 (bottom panel) where we compare experimental data ([23]) with those obtained in two different theoretical models (FRDM95 [24], HFB26 [25]). A reduction of G_n as a function of Z for heavier elements is observed in the experimental data, supporting the above discussed weakening of the shell closure inferred on the basis of the trends of δ^2-values. G_n-values are significantly reduced when crossing $Z=82$, which can be attributed to the loss of the magic $Z=82$ partner, which leads to less stable semi-magic nuclei with ^{218}U being the most unstable $N=126$ isotone known to date.

The predictive power of different theoretical models concerning the weakening of the shell closure can be tested by comparing their G_n-values to the experimental ones. The macroscopic-microscopic FRDM95 model predicts well the G_n-values around the doubly magic ^{208}Pb, but fails to describe the decreasing trend for heavier elements. On the other hand, the purely microscopic HFB26 model performs worse around ^{208}Pb, but predicts the reduction of G_n towards heavier elements better. The anomalous behaviour observed in U may thus hint at significant changes in its structure, for instance non-negligible deformation as discussed theoretically in Ref. [26], which may occur because of the weakening of the $N=126$ shell closure. To date, no experimental data on deformations of $N=124$-130 isotones are available for Po-U, except for ^{218}Ra ($N=130$), where the quadrupole deformation is 0.091(4) [9].

In conclusion, we report the discovery of the isotope ^{221}U as well as unambiguous identification of ^{222}U. Half-lives of 4.7(7)μs and 0.66(14)μs and α-particle energies of 9.31(5) MeV and 9.71(5) MeV were measured for ^{222}U and ^{221}U, respectively. These were produced in the fusion-evaporation reaction ^{50}Ti + ^{176}Yb with maximum cross sections of a few nanobarns at 47 and 54 MeV excitation energies of ^{226}U* [22]. The comparative analysis of the reduced widths and neutron-shell gaps of the Po-U isotopes show a significant weakening of the influence of the $N=126$ shell closure in U. Our findings motivate further investigations of the $N=126$ shell closure by synthesizing hitherto unknown nuclei, and by detailed studies of U. The experimental technique applied in the present work allows the identification of short-lived activities in a wide range of the nuclear chart and particularly for the still unobserved ^{220}U for which, though, the predicted half-life is only several tens of ns [10] and hence too short for surviving the flight time through TASCA. A preferable way to synthesize this isotope would be via its significantly longer lived [27] α-decay precursor ^{224}Pu.

We are grateful to GSI's ion-source and UNILAC staff. This work was in part financially supported by the Swedish Research Council.

[1] M. Pfützner, M. Karny, L.V. Grigorenko, and K. Riisager, Rev. Mod. Phys. **84**, 567 (2012).
[2] O. Sorlin and M.-G. Porquet, Prog. Part. Nucl. Phys. **61**, 602 (2008).
[3] K. Heyde and J.L. Wood, Rev. Mod. Phys. **83**, 1467 (2011).
[4] B.A. Brown, Prog. Part. Nucl. Phys. **47**, 517 (2001).
[5] H.J. Mang, Ann. Rev. Nucl. Sci. **14**, 239 (1964).
[6] J.O. Rasmussen, Phys. Rev. **113**, 1593 (1959).
[7] A.N. Andreyev et al., Phys. Rev. Lett. **110**, 242502 (2013).
[8] K.S. Toth et al., Phys. Rev. C **60**, 011302 (1999).
[9] http://www.nndc.bnl.gov/ensdf/
[10] G. Audi et al., Chinese Phys. C **36**, 1157 (2012).
[11] L. Ma et al., Phys. Rev. C **91**, 051302(R) (2015).
[12] R. Hingmann, H.-G. Clerc, C.-C. Sahm, D. Vermeulen, K.-H. Schmidt, J. G. Keller, Z. Phys. A **313** 141 (1983).
[13] K. Nishio et al., Phys. Rev. C **62** 014602 (2000).
[14] A. Semchenkov et al., Nucl. Instrum. Methods Phys. Res., Sect. B **266**, 4153 (2008).
[15] J.M. Gates et al., Phys. Rev. C **83**, 054618 (2011).
[16] W. Reisdorf, Z. Phys. A **300**, 227 (1981).
[17] E. Jäger et al., J. Radioanal. Nucl. Chem. **299**, 1073 (2014).
[18] K.E. Gregorich, Nucl. Instrum. Methods Phys. Res. Sect. A **711**, 47 (2013).
[19] J. Khuyagbaatar et al., Nucl. Instrum. Methods Phys. Res. Sect. A **689**, 40 (2012).
[20] J. Khuyagbaatar et al., Phys. Rev. A **88**, 042703 (2013).
[21] N. Kurz et al., GSI Scientific Report 252 (2012) and J. Hoffmann et al., GSI Scientific Report 253 (2012).
[22] J. Khuyagbaatar et al., to be published.
[23] M. Wang et al., Chinese Phys. C **36**, 1603 (2012).
[24] P. Möller et al., At. Data and Nuc. Data Tables **59**, 185 (1995).
[25] S. Goriely et al., Phys. Rev. C **88**, 024308 (2013).
[26] http://arxiv.org/abs/1406.7095v1
[27] P. Möller et al., At. Data and Nuc. Data Tables **66**, 131 (1997).